Original Research

A Diffusion Tensor Imaging Group Study of the Spinal Cord in Multiple Sclerosis Patients With and Without T_2 Spinal Cord Lesions

Wim Van Hecke, PhD,[1,2]* Guy Nagels, MD, PhD,[3–5] Griet Emonds, MSc,[2,6] Alexander Leemans, PhD,[7,8] Jan Sijbers, PhD,[1] Johan Van Goethem, MD, PhD,[2] and Paul M. Parizel, MD, PhD[2]

Purpose: To examine the T_2-normal appearing spinal cord of patients with multiple sclerosis (MS) using diffusion tensor imaging.

Materials and Methods: Diffusion tensor images of the spinal cord were acquired from 21 healthy subjects, 11 MS patients with spinal cord lesions, and 10 MS patients without spinal cord lesions on the T_2-weighted MR images. Different diffusion measures were evaluated using both a region of interest (ROI) -based and a diffusion tensor tractography-based segmentation approach.

Results: It was observed that the FA, the transverse diffusivity $\lambda_\perp$, and the ratio of the longitudinal and transverse diffusivities ($\lambda_\parallel/\lambda_\perp$) were significantly lower in the spinal cord of MS patients with spinal cord lesions compared with the control subjects using both the ROI method ($P = 0.014$, $P = 0.028$, and $P = 0.039$, respectively) and the tractography-based approach ($P = 0.006$, $P = 0.037$, and $P = 0.012$, respectively). For both image analysis methods, the FA and the $\lambda_\parallel/\lambda_\perp$ values were significantly different between the control group and the MS patient group without T_2 spinal cord lesions ($P = 0.013$).

Conclusion: Our results suggest that the spinal cord may still be affected by MS, even when lesions are not detected on a conventional MR scan. In addition, we demonstrated that diffusion tensor tractography is a robust tool to analyze the spinal cord of MS patients.

Key Words: spinal cord; diffusion tensor imaging; diffusion tensor tractography; multiple sclerosis
J. Magn. Reson. Imaging 2009;30:25–34.

MULTIPLE SCLEROSIS (MS) is a chronic demyelinating disease of the central nervous system, which is characterized by both inflammatory and neurodegenerative processes. Nowadays, magnetic resonance (MR) imaging is increasingly used in the diagnosis of MS patients with spinal cord involvement (1). In addition, MR can also be useful in patients who do not have clinical spinal cord involvement, because asymptomatic spinal cord lesions are common in MS and uncommon in other WM disorders (2). However, the spinal cord lesion information as obtained by a conventional MR examination does not always correlate well with the clinical disability of the patient and/or with histological information (3–5). It has been demonstrated that the white matter (WM) regions that appear normal on conventional MR images, referred to as normal-appearing WM (NAWM), are also involved in the MS disease process (6–8). In this context, diffusion tensor imaging (DTI) can provide complementary diagnostic information regarding the microstructural WM organization in MS lesions and NAWM (8,9). This technique is based on the fact that water molecules have a larger probability to diffuse along the axonal structures than perpendicular to them. Recent studies demonstrate the potential of quantitative DTI parameters, such as the fractional anisotropy (FA), which is a normalized measure of the degree of anisotropy, and the mean diffusivity (MD), that is, the averaged diffusion, for detecting WM alterations in patients with MS (10–14).

Because the spinal cord is frequently involved in MS, DTI can be regarded as a valuable technique to examine

[1]Visionlab (Department of Physics), University of Antwerp, Antwerp, Belgium.
[2]University Hospital Antwerp (Department of Radiology), University of Antwerp, Antwerp, Belgium.
[3]Department of Neurology and Memory Clinic, Middelheim General Hospital, Antwerp, Belgium.
[4]Department of Neurology, National Multiple Sclerosis Centre, Melsbroek, Belgium.
[5]Laboratory of Neurochemistry and Behavior, Institute Born-Bunge, University of Antwerp, Antwerp, Belgium.
[6]Department of Management, University of Antwerp, Antwerp, Belgium.
[7]CUBRIC (Department of Psychology), Cardiff University, Cardiff, United Kingdom.
[8]Department of Radiology, Image Science Institute, University Medical Center Utrecht, Utrecht, The Netherlands.
*Address reprint requests to: W.v.H., Vision Lab, Department of Physics, University of Antwerp, Universiteitsplein 1, N 1.18, B-2610 Antwerpen, Belgium. E-mail: wim.vanhecke@ua.ac.be
Received August 25, 2008; Accepted April 13, 2009.
DOI 10.1002/jmri.21817
Published online in Wiley InterScience (www.interscience.wiley.com).

WM alterations in the spinal cord of patients with MS. However, in contrast to the potential of such a DTI study of the spinal cord, only a limited number of papers are published regarding this topic (15–22). In this context, it is known that several factors hamper a robust DTI study of the spinal cord, such as restricted diffusion tensor (DT) image resolution, the small size of the spinal cord, and artifacts related to cardiac and respiratory motion, and magnetic field inhomogeneities (23,24). As a result, a relatively large number of voxels contain a combined signal originating from both the spinal cord and the cerebrospinal fluid (CSF), which is also known as a partial volume effect (PVE) (25).

In a preliminary study of three MS patients, Clark et al demonstrated a significant FA decrease and MD increase in MS cord lesions using a region of interest (ROI) -based approach (15). To increase the robustness and the reproducibility of the image processing, Valsasina et al and Agosta et al performed a histogram analysis on the central slice of the sagittal images (16,17). In these studies, a significant FA decrease was observed in the cervical spinal cord of MS patients, compared with healthy subjects. This histogram analysis approach was also adopted by Benedetti et al in a DTI study of MS patients and patients with neuromyelitis optica (18). Hesseltine et al. reported a significant FA decrease in the NAWM of patients with MS in the lateral, central, and posterior regions of the spinal cord at the C2–C3 level compared with healthy subjects (19). Their image processing method was based on the manual placement of circular ROIs on a single axial slice. Ohgiya et al demonstrated a reduced FA in lesions and NAWM regions of MS patients compared with healthy subjects by manually placing small, ovoid ROIs at the C2–C3, C3–C4, and C4–C5 level (20). Recently, Ciccarelli et al demonstrated that the FA is reduced in MS patients compared with normal controls, using diffusion tensor tractography (21).

Previous DTI studies of the spinal cord in MS patients focused on the examination of diffusion measures in spinal cord lesions or in NAWM near these lesions using ROIs. We hypothesize that the spinal cord can also be involved in the disease when no lesions are reported on the conventional MR scans. In addition, we hypothesize that a tractography-based spinal cord segmentation method is more reliable and sensitive to detect diffusion alterations in the normal appearing spinal cord of MS patients compared with the generally applied ROI approach (26). The aim of this work was, therefore, to examine the spinal cord diffusion properties of MS patients without T_2 spinal cord lesions using diffusion tensor tractography. To the best of our knowledge, this is the first quantitative DTI study of the cervical spinal cord that appears entirely normal on a conventional MR examination in patients with MS.

METHODS

Subjects

Diffusion tensor measurements of the cervical spinal cord (C1–C5) were acquired from 21 MS patients (age: 38 ± 9 years; 8 males, 13 females). 21 sex- and age-matched healthy subjects were additionally scanned (age: 40 ± 10 years; 8 males, 13 females). All healthy subjects had a normal appearing spinal cord on conventional T_2-weighted MR images. An informed consent was signed by all participants.

In 11 of the MS patients, which we will refer to as MS patient group 1, one or more lesions were detected in the spinal cord on conventional MR images. In the other 10 MS patients, which will be referred to as MS patient group 2, no spinal cord lesions were detected on the conventional MR scan. Twelve patients had relapse-remitting MS (6 in MS patient group 1 and 6 in MS patient group 2), 9 patients had secondary progressive MS (5 in MS patient group 1 and 4 in MS patient group 2). There was no clinical suspicion of an acute MS attack in any of the patients at the time of imaging.

MRI Acquisition

Axial diffusion tensor images were obtained on a 1.5 Tesla (T) MR scanner (Siemens, Erlangen, Germany) using a single-shot SE-EPI sequence with the following acquisition parameters: TR: 10.4 s; TE: 100 ms; diffusion gradient: 40 mT/m; FOV = 256 × 256 mm^2 matrix size: 128 × 128; number of slices = 30; image resolution = 2 × 2 × 2 mm^3; b = 700 s/mm^2; acquisition time: 12 min 18 s. Diffusion measurements were performed along 60 directions (+ 10 nondiffusion weighted (b0) images) for a robust estimation of FA, tensor orientation, and MD (27). The diffusion tensors were nonlinearly estimated based on the Levenberg-Marquardt optimization method (27).

Parallel imaging, integrating a combination of two elements of the CP (circular polarization) spine coil and one element of the neck coil, was used to reduce the effect of distortions on the data (28,29). Although magnetic susceptibility variations may not be significant deep inside the brain, they can constitute a real problem near the spinal cord. To quantify the effect of these susceptibility variations, magnetic field maps were acquired for each subject. The field map gives a direct representation of the static field inhomogeneity, allowing the measurement of the spatial misregistration associated with each point of an image. This field map was obtained by computing the phase difference between two images acquired with different echo times (30,31). When these distortions exceeded 1 voxel in the tissue of interest, as calculated from the field maps, the data set was excluded from the analysis. A linear or nonlinear image registration to correct for motion artifacts and geometrical distortions was not included in this study, because the limited image information did not allow a robust registration. Instead, all data sets were analyzed visually to check for distortions. As a result, data sets of 2 subjects were excluded from the analysis due to a significant signal dropout.

An example of the diffusion weighted images is provided in Figure 1. A contour that delineates the spinal cord is drawn on a sagittal slice of the FA map. Exactly the same contour is also placed on the same sagittal slice of the nondiffusion weighted image, the first DW image, the mean DW image, and the MD map. Diffusion tensor estimation, tractography, visualization, and

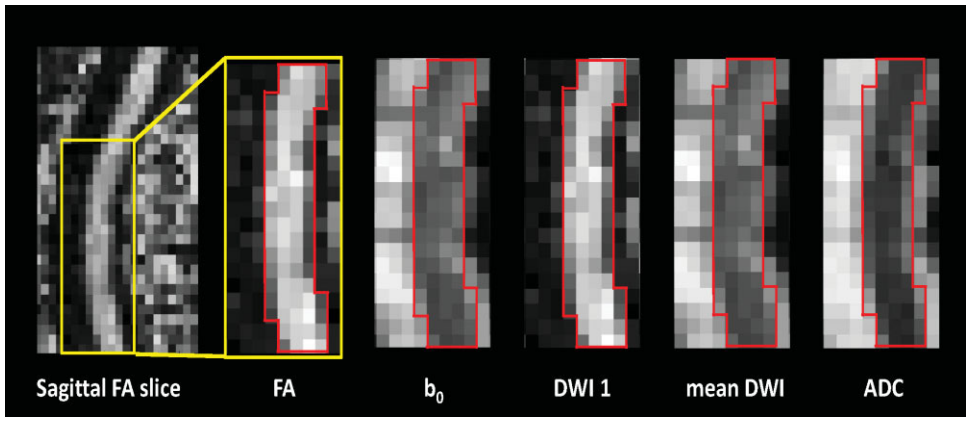

Figure 1. A contour that delineates the spinal cord is drawn in red on a sagittal slice of the FA map, the nondiffusion weighted image, the first diffusion weighted image, the mean diffusion weighted image, and the MD map. The FOV of the first image is 44 × 62 mm^2. [Color figure can be viewed in the online issue, which is available at www.interscience.wiley.com.]

quantitative analysis, was performed with the diffusion toolbox "ExploreDTI" (http://www.ExploreDTI.com) (32).

Diffusion Parameters of Interest

Multiple quantitative diffusion parameters were analyzed in all subjects. FA and MD were calculated and averaged over all selected voxels for all subjects. In addition, the longitudinal ($\lambda_{\parallel}$) and transverse ($\lambda_{\perp}$) diffusivities, and the ratio of the longitudinal versus transverse diffusivities ($\lambda_{\parallel}/\lambda_{\perp}$) were also computed, because it has been suggested that this ratio can better differentiate between healthy and diseased subjects (33–36).

Image Analysis

It is generally known that it is difficult to determine spinal cord diffusion measures, because many voxels at the edge of the spinal cord contain a signal of both the spinal cord tissue and CSF. In a first image analysis approach, ROIs were manually placed on each axial slice, thereby carefully delineating the spinal cord to avoid the inclusion of PVE contaminated voxels in the analysis. All ROIs were defined on the axial slices of the FA maps, color encoded for the diffusion direction, because they provided the best contrast between the spinal cord tissue and the surrounding CSF (see Fig. 2a,b).

In a second image analysis method, also referred to as the tract-based segmentation approach, diffusion tensor tractography was performed on the spinal cord that was first manually delineated by ROIs (see Fig. 2c) (26). A standard deterministic streamline-based fiber tracking approach was applied with only one seed point per voxel in which the step size was 1 mm (37). The maximal angle between two consecutive tract directions was set to 20° and an FA threshold of 0.3 was used during tractography, as in Van Hecke et al (26), Tsuchiya et al (38) and Melhem et al (39). Subsequently, all quantitative diffusion parameters of interest are selected on the tracts. The tractography parameters were defined as in Van Hecke et al, and a careful visual inspection was performed to make sure that the whole spinal cord was covered by fiber tracts without any interruptions in all subjects (26). Diffusion tensor tractography is thus used to further segment the spinal cord tissue, using the orientational diffusion information that is present in each voxel. The spinal cord was thereby initially separated from the background noise by drawing an ROI on every axial slice. Multiple ROIs were used to make sure the whole cervical spinal cord was included in the analysis.

The diffusion properties of the MS lesions and the NAWM in the patients with MS lesions were also evaluated. The MS lesions were identified on the anatomical MR images that were acquired at exactly the same cord levels as the diffusion tensor data sets. The ROIs that were used to delineate the lesions on the anatomical MR images were transferred to the DTI data set to obtain the diffusion properties. Analogously, ROIs were drawn on the conventional MR images to delineate the NAWM tissue and subsequently transferred to the DTI data set. As in the work of Filippi et al., spinal cord tissue was assigned to be normal appearing when no lesion was found in the adjacent slices (40).

Statistical Analysis Procedures

Statistical tests were performed with the SPSS analysis package (http://www.spss.com). Male and female data sets were combined because a t-test showed no difference in any of the diffusion parameters between both sexes ($P >> 0.05$, with 16 males versus 26 females). Moreover, the age distribution in the three subject groups was not significantly different for both sexes ($P >> 0.05$, with 16 males versus 26 females).

An analysis of covariance (ANCOVA) was used to compare the cervical cord diffusion properties from the control subject group with both MS patient groups. Kolmogorov-Smirnov tests demonstrated that a parametric approach could be applied ($P >> 0.05$). Potentially confounding factors, such as the subject's age and the cross-sectional area of their cervical spinal cord—measured as the number of selected voxels—were included in the ANCOVA model. Although the age and the cross-sectional area were not differently distributed in the different subject groups, both factors were included in the analysis of covariance. Differences in diffusion measures between groups could, therefore, be attributed to an intrinsic difference between the diffusion properties of the subjects groups. In this context, the cervical spinal cord cross sectional area A was calculated separately for both image analysis approaches

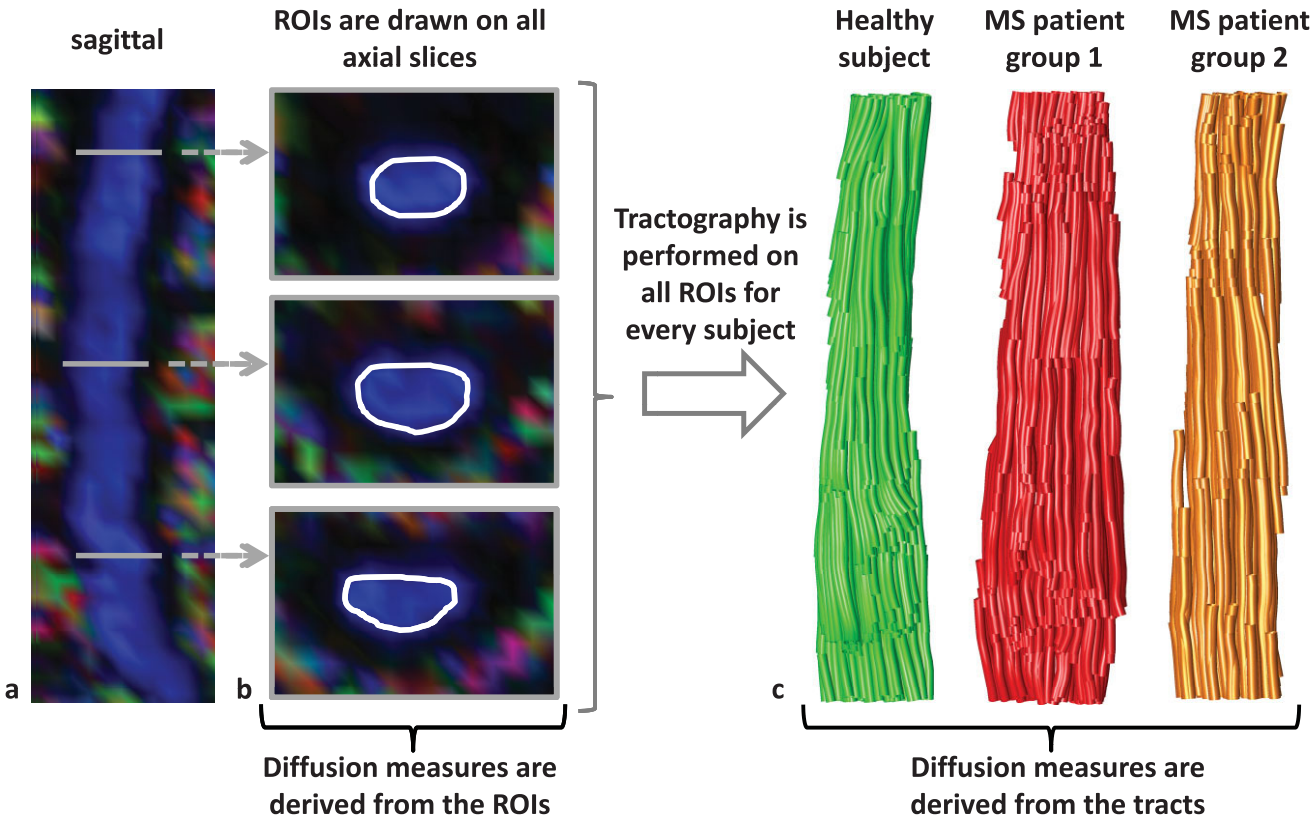

Figure 2. **a:** A sagittal slice of the spinal cord. The color is encoded for the diffusion direction, and the intensity is proportional with the diffusion anisotropy. **b:** In the ROI-based segmentation method, ROIs are drawn on all axial slices, as demonstrated for three axial slices. In the tractography-based segmentation method, diffusion measures are derived from the tracts. **c:** The tractography result of a healthy subject an MS patient with T_2 spinal cord lesions and an MS patient without T_2 spinal cord lesions are visualized. [Color figure can be viewed in the online issue, which is available at www.interscience.wiley.com.]

as the number of selected voxels for analysis. In addition, the statistical results were adjusted to correct for multiple comparisons using Fisher's least significant difference approach.

The intra-observer reproducibility of the different image analysis methods was tested using the intra-class correlation coefficient (ICC). To this end, the ROIs were drawn a second time by the same observer. A measurement is deemed highly reproducible if ICC > 0.9. In the case of $0.7 <$ ICC < 0.9, the reproducibility is considered acceptable. Finally, results with an ICC < 0.7 are interpreted as poorly reproducible.

RESULTS

Using the ROI approach, a mean cross sectional surface A of 80.3 mm^2, 70.7 mm^2, and 75.4 mm^2 was observed for the control group, the MS patient group with lesions, and the MS patient group without spinal cord lesions, respectively (see Table 1; Fig. 3). Although larger cross

Table 1
Diffusion Values Average A, FA, MS, $\lambda_{\parallel}$, $\lambda_{\perp}$, and $\lambda_{\parallel}/\lambda_{\perp}$ are Displayed Using Three Different Spinal Cord Segmentation Approaches in Control Subjects, MS Patients with Plaques in the Spinal Cord, and MS Patients Without Plaques in the Spinal Cord.

Average (Standard Deviation)	Control subjects		MS patients with plaques in the spinal cord		MS patients without plaques in the spinal cord	
	ROI	TS	ROI	TS	ROI	TS
A	80.3 (7.3)	89.2 (9.2)	70.7 (10.0)	79.9 (9.3)	75.4 (10.2)	82.0 (10.1)
FA	0.58 (0.03)	0.53 (0.03)	0.54 (0.04)	0.48 (0.05)	0.55 (0.05)	0.48 (0.04)
MD $\times 10^{-3}$ mm^2/s	1.09 (0.10)	1.21 (0.11)	1.23 (0.05)	1.31 (0.10)	1.18 (0.09)	1.24 (0.06)
$\lambda_{\parallel}$ $\times 10^{-3}$ mm^2/s	1.89 (0.17)	2.02 (0.19)	2.04 (0.24)	2.18 (0.23)	1.97 (0.21)	2.10 (0.22)
$\lambda_{\perp}$ $\times 10^{-3}$ mm^2/s	0.69 (0.08)	0.86 (0.08)	0.83 (0.09)	0.96 (0.07)	0.79 (0.08)	0.92 (0.06)
$\lambda_{\parallel}/\lambda_{\perp}$	2.76 (0.16)	2.38 (0.08)	2.47 (0.14)	2.21 (0.10)	2.51 (0.15)	2.23 (0.09)

Abbreviations: A: cross-sectional spinal cord area; FA: fractional anisotropy; MD: mean diffusivity; $\lambda_{\parallel}$: longitudinal diffusivity; $\lambda_{\perp}$: transverse diffusivity; ROI: region of interest; TS: tract based segmentation method

sectional areas of 89.2 mm^2, 79.9 mm^2, and 82.0 mm^2 were found for the different subject groups using the tractography-based image analysis method (see Table 1; Fig. 3), Pearson correlation tests demonstrated a significant correlation between the cross sectional areas of the ROI- and the tractography-based approach ($P << 0.001$; $r > 0.9$, results not shown). These results suggest that a smaller cross sectional area of the spinal cord can be observed in the MS patient groups compared with the control group. However, this difference was not found to be statistically significant, as can be observed in Table 2.

The cervical spinal cord diffusion metrics of the different subject groups are presented for the ROI- and the tractography-based image analysis approaches in Table 1. The distribution of these diffusion measures is visualized using boxplots in Figure 3, whereby the boxplots of the control group, the MS group with spinal cord lesions, and the MS group without known spinal cord lesions are colored in green, red, and orange, respectively. The results of ANCOVA tests, which compare the diffusion measures across the different subject groups, thereby taking into account the subject age and the cross-sectional spinal cord area, are displayed in Table 2. It can be observed that the FA, the transverse diffusivity $\lambda_{\perp}$, and the ratio of the longitudinal and transverse diffusivities ($\lambda_{\parallel}/\lambda_{\perp}$) are significantly lower for the MS patients with spinal cord lesions compared with the control subjects using the ROI method ($P = 0.014$, $P = 0.028$, and $P = 0.039$, respectively) and the tractography-based approach ($P = 0.006$, $P = 0.037$, and $P = 0.012$, respectively). Although the visual results of Figure 3 suggest an increased MD in the MS patient group with spinal cord lesions, no statistically significant difference in MD was found (Table 2).

The FA and the $\lambda_{\parallel}/\lambda_{\perp}$ values were significantly different between the control group and the MS patient group without spinal cord lesions. These FA differences are statistically significant with a P value of 0.013 for both image analysis methods (Table 2). For $\lambda_{\parallel}/\lambda_{\perp}$, a P value of 0.018 and 0.020 was found for the ROI- and the tractography-based method, respectively. The diffusion values of the MS patients without spinal cord lesions were not observed to be different from the diffusion measures of the MS patients with spinal cord lesions (see Fig. 1, statistical results not shown). In addition to the study of the NAWM of MS patients without spinal cord lesions, the NAWM diffusion measures of MS patients with spinal cord lesions are examined. To this end, the lesions and the NAWM were separated manually by ROIs. As can be observed in Table 4, all diffusion measures are significantly different in the spinal cord plaques compared with the measures of the control subjects.

No statistical difference was observed between the cervical spinal cord diffusion measures of patients with and patients without spinal cord lesions using both postprocessing methods ($P >> 0.05$). In addition, no diffusion differences were found between the NAWM of the patients with and without spinal cord lesions.

Finally, the reproducibility of image processing methods is examined using the intra-class correlation coefficient. As can be observed in Table 3, the ICC is very high for the tractography-based method. Because the ROI approach is more user dependent due to the manual delineation of the ROIs, lower ICC values were observed (see Table 3). Although these ICC values (0.66–0.85) represent an acceptable reproducibility, the observer-dependency affects the statistical results of the ROI analysis (see Table 2).

DISCUSSION

Conventional MR is used in daily clinical routine to detect spinal cord lesions in patients with MS. However, it has been demonstrated that findings on conventional MR scans do not always correlate well with the clinical status of the MS patients (41,42). In addition, previous studies did not find a correlation between the clinical disability of MS patients and the number and extent of the spinal cord lesions that were detected on MR (43–46). Because DTI provides information about the microstructural WM organization, the resulting diffusion metrics are potentially more sensitive to detect spinal cord involvement in MS patients than conventional MR is.

In this work, the spinal cord of MS patients without any lesions on the conventional MR scans is studied with DTI. To the best of our knowledge, all DTI studies of the spinal cord in MS patients evaluated the diffusion metrics in spinal cord lesions or in NAWM in the proximity of lesions. Our results suggest that the FA and the ratio of the longitudinal and transverse eigenvalues are significantly reduced in the spinal cord of MS patients without lesions (see Fig. 3; Tables 1, 2). These results were confirmed by the analysis of the NAWM in the spinal cord with lesions (see Table 4). In concordance with the literature, the FA was found to be significantly reduced in the MS patients with spinal cord lesions compared with the FA of the age- and sex-matched control subjects (15–22). In addition, a significant increase of the transverse eigenvalues and decrease of the ratio of the longitudinal and transverse eigenvalues was observed in the spinal cord of these MS patients compared with the control subjects. Within the spinal cord lesions, the FA and the ratio of the longitudinal and transverse eigenvalues were decreased and the MD, the longitudinal, and transverse eigenvalues were increased, compared with the diffusion measures of the healthy spinal cord tissue of the control subjects.

In agreement with the literature, our results suggest that the FA and the ratio of the longitudinal and transverse diffusivities are the most sensitive diffusion measures to detect microstructural alterations that are induced by the MS disease process. These differences were observed in the NAWM and the lesions of MS patients with T_2 spinal cord lesions and in the NAWM of MS patients without T_2 spinal cord lesions (see Tables 2, 4). Additionally, an increased MD, longitudinal diffusivity, and transverse diffusivity was observed within the spinal cord lesions. A recent postmortem study, which correlated diffusion measures with the myelin content and the axonal count, suggested that an FA decrease and a MD increase is primary correlated with loss of myelin (47). Recent studies using animal models further demonstrated that a loss of axons is repre-

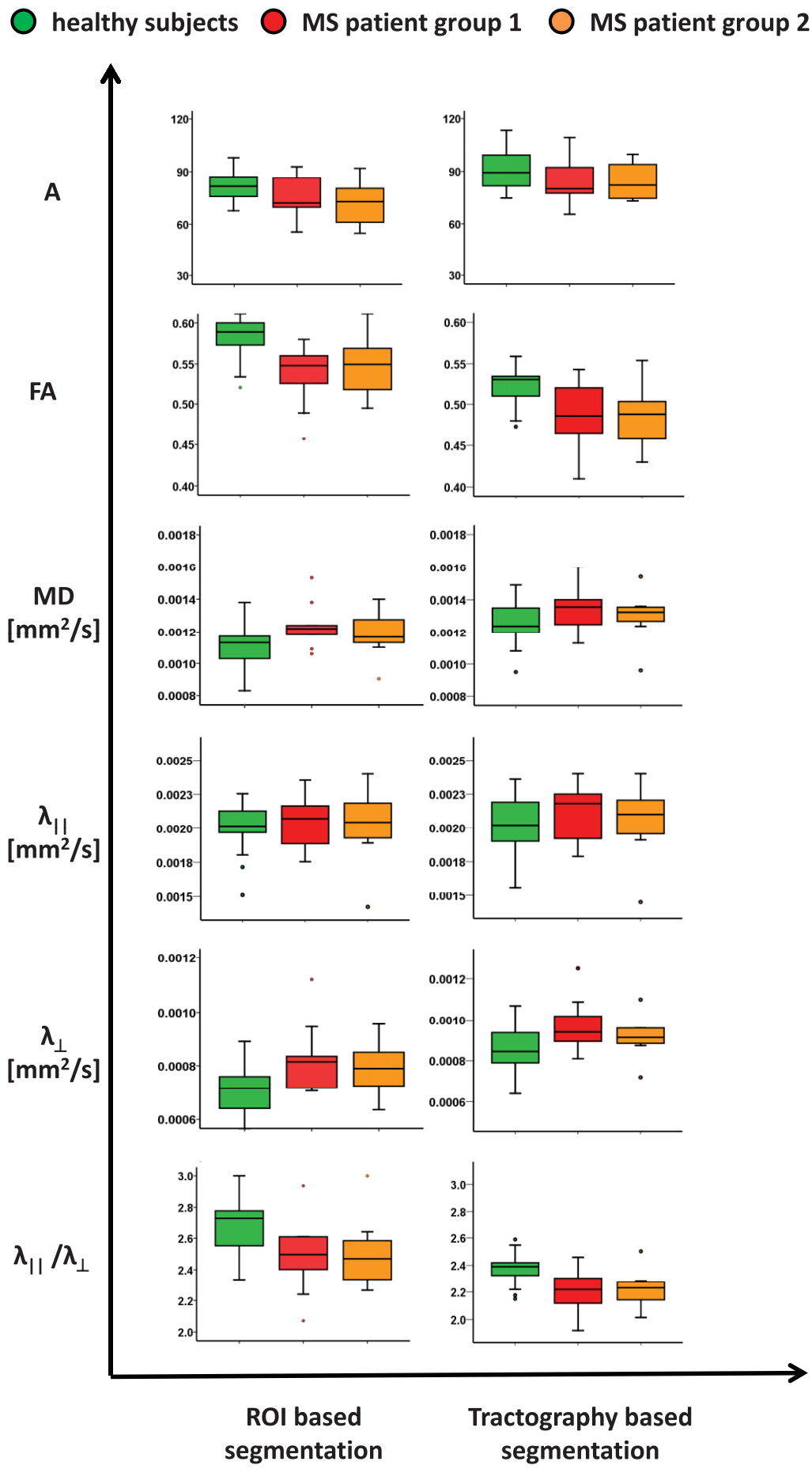
healthy subjects
MS patient group 1
MS patient group 2
A
FA
MD [mm²/s]
λ|| [mm²/s]
λ⊥ [mm²/s]
λ|| /λ⊥
ROI based segmentation
Tractography based segmentation

Figure 3.

Table 2
Statistical Results (p-Values) of the Comparision of the Diffusion Measures Between the Control Group and Both the MS Patient Groups

	Control subjects vs MS patients with plaques in the spinal cord			Control subjects vs MS patients without plaques in the spinal cord		
	ROI[c]	ROI[d]	TS	ROI[c]	ROI[d]	TS
A[a]	0.283	0.114	0.174	0.090	0.078	0.168
FA[b]	**0.014**	0.119	**0.006**	**0.013**	0.058	**0.013**
MD[b]	0.063	0.235	0.138	0.353	0.461	0.584
$\lambda_{\parallel}$[b]	0.192	0.385	0.350	0.607	0.681	0.930
$\lambda_{\perp}$[b]	**0.028**	0.209	**0.037**	0.258	0.371	0.155
$\lambda_{\parallel}/\lambda_{\perp}$[b]	**0.039**	0.139	**0.012**	**0.018**	0.111	**0.020**

[a]ANOVA analysis, corrected for multiple comparisons using Fisher's least significant difference method
[b]ANCOVA analysis, corrected for the cross sectional area of the spinal cord and for age, including a multiple comparisons correction based on Fisher's least significant difference method
[c]Results of the first ROI delineation analysis
[d]Results of the second ROI delineation analysis by the same observer as the first ROI analysis
Abbreviations: A: cross-sectional spinal cord area; FA: fractional anisotropy; MD: mean diffusivity; $\lambda_{\parallel}$: longitudinal diffusivity; $\lambda_{\perp}$: transverse diffusivity; ROI: region of interest; TS: tract based segmentation method
Note: The statistically significant values are bold.

sented by a decreased longitudinal diffusivity and a normal transverse diffusivity, whereas myelin breakdown is represented by an increased transverse diffusivity and a normal longitudinal diffusivity (33–36). Another postmortem study demonstrated a strong correlation of the axonal density and loss of myelin with the diffusion anisotropy and a weaker correlation with the MD (48). As also proposed by Agosta et al, astrocytic proliferation, cell debris, fibrillary gliosis, and inflammatory infiltrates can result in a normalization of the MD values and can, therefore, prevent the MD differences to be statistically significant, as observed in our study (17,22,49). Some studies report differences in the diffusion measures between relapse-remitting, primary-progressive and secondary-progressive MS patients (16,22). In our study, the diffusion properties were not found to be statistically different between the subjects with relapse-remitting MS and secondary-progressive MS, which might be explained by the low statistical power due to the limited number of patients in our study.

We did not observe a statistical difference between the different cervical spinal cord diffusion measures of MS patients with and without spinal cord lesions, using the ROI as well as the tractography segmentation method. This suggests that the microstructural damage in the spinal cord of MS patients is not significantly different in patients with lesions compared with patients without lesions. Here, we want to stress that our results should be interpreted cautiously, given that our study may have been limited by the relatively small number of subjects.

Figure 3. Boxplots are shown for the cross-sectional spinal cord area A, the fractional anisotropy, the mean diffusivity, the longitudinal and the transverse diffusivities, and for the ratio of the longitudinal and transverse eigenvalues. Results of both segmentation methods are displayed for the control subjects, the MS patients with T_2 spinal cord lesions (MS patient group 1), and the MS patients without T_2 spinal cord lesions (MS patient group 2).

Table 3
Reproducibility Intra-Class Correlation Coefficients (ICC) Measure the Intra-Rater Reproducibility of the Different Diffusion Measures

ICC	ROI	TS
FA	0.79	0.96
MD $\times 10^{-3}$ mm^2/s	0.79	0.97
$\lambda_{\parallel}$ $\times 10^{-3}$ mm^2/s	0.85	0.97
$\lambda_{\perp}$ $\times 10^{-3}$ mm^2/s	0.83	0.98
$\lambda_{\parallel}/\lambda_{\perp}$	0.66	0.96

Abbreviations: FA: fractional anisotropy; MD: mean diffusivity; $\lambda_{\parallel}$: longitudinal diffusivity; $\lambda_{\perp}$: transverse diffusivity; ROI: region of interest; TS: tract based segmentation method

The magnitude of the quantitative diffusion measures that were found in this study (see Table 1), are within the range of the previously reported values (see Table 5). Notice that a large variability exists in the FA and MD measures across different studies (15–21). This is probably due to disease heterogeneity in the different groups (different age range, disease state, and so on), the use of different image acquisition and analysis methods, and the relatively low reproducibility of some of these methods. All previous DTI studies of the spinal cord of MS patients reported a statistically significant FA difference between the control group and the MS patient group, whereas MD was only found to be different in some studies. In addition to the group and disease heterogeneity and the use of various image analysis methods, the application of different statistical methods and post hoc tests, and the incorporation of various cofactors in the statistics can explain the differences in the reported *P* values. Different cofactors, such as the age of the subjects and the cross-sectional area of the spinal cord were incorporated in the statis-

Table 4
Control Diffusion Measures vs. Plaques and NAWM

	Control vs plaques	Control vs NAWM
FA	0.001	0.012
MD $\times 10^{-3}$ mm^2/s	0.017	0.175
$\lambda_{\parallel}$ $\times 10^{-3}$ mm^2/s	0.035	0.761
$\lambda_{\perp}$ $\times 10^{-3}$ mm^2/s	0.005	0.071
$\lambda_{\parallel}/\lambda_{\perp}$	0.011	0.035

Diffusion measures in the plaques of the MS patients are compared with diffusion measures of the control subjects (p-values in left column). In addition, the diffusion metrics of the control subjects are compared with these of the NAWM in the MS patients with spinal cord lesions (p-values in right column). ROIs were used for this analysis.
Abbreviations: FA: fractional anisotropy; MD: mean diffusivity; $\lambda_{\parallel}$: longitudinal diffusivity; $\lambda_{\perp}$: transverse diffusivity; NAWM: normal appearing white matter

Table 5
Comparison with Literature: Comparison of FA and MD Values Across Different DTI Studies of the Spinal Cord in MS Patients

Reference	control subjects		MS patients	
	FA	MD $\times 10^{-3}$ mm^2/s	FA	MD $\times 10^{-3}$ mm^2/s
Current study	0.58	1.09	0.55	1.21
Current study	0.53	1.21	0.48	1.28
Valsasina et al. 2005	0.43	1.22	0.36	1.28
Agosta et al. 2005	0.42	1.20	0.38	1.28
Benedetti et al. 2006	0.42	1.22	0.37	1.32
Hesseltine et al. 2006	0.60	0.82	0.52	0.88
Ohgiya et al. 2007	0.74	0.64	0.56	0.72
Cicarelli et al. 2005	0.47	0.71	0.42	0.73

Abbreviations: FA: fractional anisotropy; MD: mean diffusivity

tics because it is known that these factors can affect diffusion values of the spinal cord (26).

Because many spinal cord voxels are affected by different degrees of partial volume averaging with CSF it is not straightforward to reliably select the relevant spinal cord voxels of interest in the different subjects. Some studies evaluate histogram information originating from the central part of the spinal cord (16–18). In this approach, a lot of valuable information is discarded. In addition, the sensitivity to find differences between control subjects and MS patients can be reduced, because Hesseltine et al demonstrated that only minor differences were found in the central part of the spinal cord, which mainly consist of grey matter (19). Most of the studies use an ROI-based approach to obtain diffusion data. However, it has been demonstrated that the reproducibility of this method can be very low (26). Although the ICC values that were found in this study were acceptable (see Table 3), the statistical results and conclusions differed significantly when the ROIs were drawn a second time by the same observer (see Table 2). In this context, there is a need for a standardized approach for analyzing spinal cord DTI data, which, in our opinion, is provided by diffusion tensor tractography-based segmentation. In contrast to studies that incorporated diffusion tensor tractography results of the spinal cord to provide qualitative information regarding the fiber architecture, tractography was applied in this study to provide quantitative diffusion information regarding the WM damage induced in the spinal cord of patients with MS (38,50–54). Compared with the ROI method, an observer dependency is replaced by a parameter dependency of the tractography algorithm, resulting in a more reproducible and standardized measurement of the diffusion characteristics (see Table 3). Because the application of tractography in the spinal cord might be limited over large distances, we opted for drawing ROIs on every axial slice.

A standard acquisition scheme was used, which is available on most scanners in a clinical setting, without the need of specific hardware. In addition, isotropic voxels were acquired to reduce the PVE of spinal cord tissue with the surrounding CSF in the slice direction. However, due to the limited in-plane resolution, it was hard to separate WM and GM. In addition, other reported modifications of the DTI acquisition scheme might improve image quality and, therefore, the reliability of the subsequent analysis. For example, studies have focused on the optimization of the DTI acquisition with respect to bulk motion and pulsatile flow artifacts from the surrounding CSF (55–59). Other studies used cardiac gating and interleaved echo-planar diffusion imaging to reduce motion artifacts and scan time, respectively (60,61). Line scan imaging is a fast technique that relies on the acquisition of columns (57,62). The advantage of our work is that it uses a standard, widely available acquisition scheme with isotropic voxels. 60 diffusion directions were used to increase the SNR and the reliability of our estimated diffusion measures to perform tractography reliably (27). Another limitation of our study is that no correlation was made of the diffusion metrics with clinical symptoms, as measured for example by the Expanded Disability Status Scale (EDSS) (63). However, the primary aim of our study was to demonstrate the feasibility and potential of the tractography-based segmentation approach to evaluate the spinal cord damage of MS patients and to investigate the diffusion measures of MS patients without T_2 spinal cord lesions. The correlation of the diffusion metrics with the clinical status of the patients is already thoroughly reported in earlier studies (16–18,21). We also acknowledge the fact that some distortions might still be present in our data sets. We tried to correct for geometrical and motion distortions using a nonlinear image registration. However, such an automated correction did not lead to improved results (as determined by the residuals from the diffusion tensor fit), due to the relatively low amount of image information. In addition, no cardiac gating was used during the image acquisition.

We believe that our results demonstrate that diffusion tensor tractography has the potential to be used a standardized segmentation tool of spinal cord DT images for the interpretation of NAWM results in MS patients. We also acknowledge that our findings are by no means conclusive and that our results should be interpreted cautiously, given that our study may have been limited by the relatively small number of subjects.

In conclusion, diffusion measures of the normal appearing white matter were evaluated in MS patients without spinal cord lesions. A reduced FA and ratio of the longitudinal and the transverse eigenvalues was observed in the spinal cord of MS patients without any detected spinal cord lesion on a conventional MR scan. These results, therefore, suggest that the spinal cord is not preserved in MS when lesions are only detected in the brain. Furthermore, this confirms previous findings, which demonstrated that DTI is more sensitive compared with conventional MR imaging in assessing the tissue damage in MS patients. In addition, we demonstrated that diffusion tensor tractography is a robust tool to analyze the spinal cord of MS patients and that the use of tractography is more reproducible and reliable compared with an ROI analysis to evaluate the diffusion measures of the spinal cord.

REFERENCES

1. Agosta F, Filippi M. MRI of spinal cord in multiple sclerosis. J Neuroimag 2007;17(Suppl 1):46S–49S.

2. Bot JC, Barkhof F, Polman CH, et al. Spinal cord abnormalities in recently diagnosed MS patients: added value of spinal MRI examination. Neurology 2004;62:26–33.
3. Kidd D, Thorpe J, Thompson A, et al. Spinal cord MRI using multiarray coils and fast spin echo. II. Findings in multiple sclerosis. Neurology 1993;43:2632–2637.
4. Bjartmar C, Kinkel RP, Kidd G, et al. Axonal loss in normal-appearing white matter in a patient with acute MS. Neurology 2001;57: 1248–1252.
5. Tartaglino L, Friedman D, Flanders A, Lublin F, Knobler R, Liem M. Multiple sclerosis in the spinal cord: MR appearance and correlation with clinical parameters. Radiology 1995;195:725–732.
6. Miller DH, Grossman RI, Reingold SC, Mcfarland HF. The role of magnetic resonance techniques in understanding and managing multiple sclerosis. Brain 1998;121(Pt 1):3–24.
7. Werring D, Clark C, Barker G, Thompson A, Miller D. Diffusion tensor imaging of lesions and normal-appearing white matter in multiple sclerosis. Neurology 1999;52:1626–1632.
8. Rovaris M, Judica E, Gallo A. Grey matter damage predicts the evolution of primary progressive multiple sclerosis at 5 years. Brain 2006;129(Pt 10):2628–2634.
9. Cassol E, Ranjeva JP, Ibarrola D, et al. Diffusion tensor imaging in multiple sclerosis: a tool for monitoring changes in normal-appearing white matter. Mult Scler 2004;10:188–196.
10. Beaulieu C. The basis of anisotropic water diffusion in the nervous system - a technical review. NMR Biomed 2002;15:435–455.
11. Basser PJ, Jones DK. Diffusion-tensor MRI: theory, experimental design and data analysis - a technical review. NMR biomed 2002; 15:456–467.
12. Ge Y, Law M, Grossman R. Applications of diffusion tensor MR imaging in multiple sclerosis. Ann N Y Acad Sci 2005;1064:202–219.
13. Guo A, MacFall J, Provenzale J. Multiple sclerosis: diffusion tensor MR imaging for evaluation of normal-appearing white matter. Radiology 2002;222:729–736.
14. Horsfield M, Larsson H, Jones DK, Gass A. Diffusion magnetic resonance imaging in multiple sclerosis. J Neurol Neurosurg Psychiatry 1998;64(Suppl 1):S80–S84.
15. Clark CA, Werring DJ, Miller DH. Diffusion imaging of the spinal cord in vivo: estimation of the principal diffusivities and application to multiple sclerosis. Magn Reson Med 2000;43:133–138.
16. Valsasina P, Rocca MA, Agosta F, et al. Mean diffusivity and fractional anisotropy histogram analysis of the cervical cord in MS patients. NeuroImage 2005;26:822–828.
17. Agosta F, Benedetti B, Rocca MA, et al. Quantification of cervical cord pathology in primary progressive MS using diffusion tensor MRI. Neurology 2005;64:631–635.
18. Benedetti B, Valsasina P, Judica E, et al. Grading cervical cord damage in neuromyelitis optica and MS by diffusion tensor MRI. Neurology 2006;67:161–163.
19. Hesseltine SM, Law M, Babba J, et al. Diffusion tensor imaging in multiple sclerosis: assessment of regional differences in the axial plane within normal-appearing cervical spinal cord. AJNR Am J Neuroradiol 2006;27:1189–1193.
20. Ohgiya Y, Oka M, Hiwatashi A, et al. Diffusion tensor MR imaging of the cervical spinal cord in patients with multiple sclerosis. Eur Radiol 2007;17:2499–2504.
21. Ciccarelli O, Wheeler-Kingshott CA, McLean MA, et al. Spinal cord spectroscopy and diffusion-based tractography to assess acute disability in multiple sclerosis. Brain 2007;130:2220–2231.
22. Agosta F, Absinta M, Sormani MP, et al. In vivo assessment of cervical cord damage in MS patients: a longitudinal diffusion tensor MRI study. Brain 2007;130:2211–2219.
23. Clark CA, Werring DJ. Diffusion tensor imaging in spinal cord: methods and applications - a review. NMR Biomed 2002;15:578–586.
24. Wheeler-Kingshott CA, Hickman SJ, Parker GJ, et al. Investigating cervical spinal cord structure using axial diffusion tensor imaging. Neuroimage 2002;16:93–102.
25. Pfefferbaum A, Sullivan EV. Increased brain white matter diffusivity in normal adult aging: relationship to anisotropy and partial voluming. Magn Reson Med 2003;49:953–961.
26. Van Hecke W, Leemans A, Sijbers J, Vandervliet E, Van Goethem J, Parizel PM. A tracking based DTI segmentation method for the detection of diffusion-related changes of the cervical spinal cord with aging. J Magn Reson Imaging 2008;27:978–991.
27. Jones DK. The effect of gradient sampling schemes on measures derived from diffusion tensor MRI: a Monte Carlo study. Magn Reson Med 2004;51:807–815.
28. Griswold MA, Jakob PM, Chen Q, et al. Resolution enhancement in single-shot imaging using simultaneous acquisition of spatial harmonics (SMASH). Magn Reson Med 1999;41:1236–1245.
29. Bammer R, Keeling SL, Augustin M, et al. Improved diffusion-weighted singleshot echo-planar imaging (EPI) in stroke using sensitivity encoding (SENSE). Magn Reson Med 2001;46:548–554.
30. Jezzard P, Balaban RS. Correction for geometric distortion in echo planar images from B0 field variations. Magn Reson Med 1995;34: 65–73.
31. Reber PJ, Wong EC, Buxton RB, Frank LR. Correction of off resonance-related distortion in EPI using EPI-based field maps. Magn Reson Med 1998;39:328–330.
32. Leemans A, Sijbers J, Parizel PM. A graphical toolbox for exploratory diffusion tensor imaging and fiber tractography. In: Proceedings of the 14th Annual Meeting - Section for Magnetic Resonance Technologists, Miami, Florida, 2005. (abstract 345).
33. Song SK, Sun SW, Ramsbottom MJ, et al. Dysmyelination revealed through MRI as increased radial (but unchanged axial) diffusion of water. Neuroimage 2002;17:1429–1436.
34. Song SK, Sun SW, Ju W-K, et al. Diffusion tensor imaging detects and differentiates axon and myelin degeneration in mouse optic nerve after retinal ischemia. Neuroimage 2003;20:1714–1722.
35. Song SK, Yoshino J, Le TQ, et al. Demyelination increases radial diffusivity in corpus callosum of mouse brain. Neuroimage 2005; 21:132–140.
36. Pierpaoli C, Barnett A, Pajevic S, et al. Water diffusion changes in Wallerian degeneration and their dependence on white matter architecture. Neuroimage 2001;13(Pt 1):1174–1185.
37. Basser PJ, Pajevic S, Pierpaoli C, et al. In vivo fiber tractography using DT-MRI data. Magn Reson Med 2000;44:625–632.
38. Tsuchiya K, Fujikawa A, Honya K, Nitatori T, Suzuki Y. Diffusion tensor tractography of the lower spinal cord. Neuroradiology 2008; 50:221–225.
39. Melhem ER, Mori S, Mukundan G, Kraut MA, Pomper MG, van Zijl PC. Diffusion tensor MR imaging of the brain and white matter tractography. AJR Am J Roentgenol 2002;178:3–16.
40. Filippi M, Iannucci G, Cercignani M, Rocca MA, Pratesi A, Comi G. A quantitative study of water diffusion in multiple sclerosis lesions and normal-appearing white matter using echo-planar imaging. Arch Neurol 2000;57:1017–1021.
41. Lovas G, Szilagyi N, Majtenyi K, et al. Axonal changes in chronic demyelinated cervical spinal cord plaques. Brain 2000;123:308–317.
42. Bergers E, Bot JC, van der Valk P, et al. Diffuse signal abnormalities in the spinal cord in multiple sclerosis: direct postmortem in situ magnetic resonance imaging correlated with in vitro high-resolution magnetic resonance imaging and histopathology. Ann Neurol 2002;51:652–656.
43. Kidd D, Thorpe JW, Thompson AJ, et al. Spinal cord MRI using multi-array coils and fast spin echo. II. Findings in multiple sclerosis. Neurology 1993;43:2632–2637.
44. Nijeholt GJ, van Walderveen MAA, Castelijns JA, et al. Brain and spinal cord abnormalities in multiple sclerosis. Correlation between MRI parameters, clinical subtypes and symptoms. Brain 1998;121:687–697.
45. Stevenson VL, Moseley IF, Phatouros CC, et al. Improved imaging of the spinal cord in multiple sclerosis using three-dimensional fast spin echo. Neuroradiology 1998;40:416–419.
46. Stevenson VL, Leary SM, Losseff NA, et al. Spinal cord atrophy and disability in MS. A longitudinal study. Neurology 1998;51:234–238.
47. Schmierer K, Wheeler-Kingshott CA, Boulby PA, et al. Diffusion tensor imaging of post mortem multiple sclerosis brain. Neuroimage 2007;35:467–477.
48. Mottershead JP, Schmierer K, Clemence M, et al. High field MRI correlates of myelin content and axonal density in multiple sclerosis. A post-mortem study of the spinal cord. J Neurol 2003;250: 1293–1301.
49. Nijeholt GJ, Bergers E, Kamphorst W, et al. Post-mortem high-resolution MRI of the spinal cord in multiple sclerosis: a correlative study with conventional MRI, histopathology and clinical phenotype. Brain 2001;124(Pt 1):154–66.

50. Facon D, Ozanne A, Fillard P, et al. MR diffusion tensor imaging and fiber tracking in spinal cord compression. AJNR Am J Neuroradiol 2005;26:1587–1594.
51. Ducreux D, Lepeintre JF, Fillard P, et al. MR diffusion tensor imaging and fiber tracking in 5 spinal cord astrocytomas. AJNR Am J Neuroradiol 2006;27:214–216.
52. Voss HU, Watts R, Uluğ AM, Ballon D. Fiber tracking in the cervical spine and inferior brain regions with reversed gradient diffusion tensor imaging. Magn Reson Imaging 2006;24:231–239.
53. Renoux J, Facon D, Fillard P, et al. MR Diffusion tensor imaging and fiber tracking in inflammatory diseases of the spinal cord. AJNR Am J Neuroradiol 2006;27:1947–1951.
54. Vargas M, Delavelle J, Jlassi H, et al. Clinical applications of diffusion tensor tractography of the spinal cord. Neuroradiology 2008; 50:25–29.
55. Maier SE, Mamata H. Diffusion tensor imaging of the spinal cord. Ann N Y Acad Sci 2005;1064:50–60.
56. Bammer R, Fazekas F, Augustin M, et al. Diffusion-weighted MR imaging of the spinal cord. AJNR Am J Neuroradiol 2000;21:587–591.
57. Robertson RL, Maier SE, Mulkern RV, et al. MR line-scan diffusion imaging of the spinal cord in children. AJNR Am J Neuroradiol 2007;21:1344–1348.
58. Chou M-C, Lin Y-R, Huang T-Y, et al. FLAIR diffusion-tensor MR tractography comparison of fiber tracking with conventional imaging. AJNR Am J Neuroradiol 2005;26:591–597.
59. Carballido-Gamio J, Xu D, Newitt D, Han ET, Vigneron DB, Majumdar S. Single-shot fast spin-echo diffusion tensor imaging of the lumbar spine at 1.5 and 3 T. Magn Reson Imaging 2007;25:665–670.
60. Summers P, Staempfli P, Jaermann T, et al. A preliminary study of the effects of trigger timing on diffusion tensor imaging of the human spinal cord. AJNR Am J Neuroradiol 2006;27:1952–1961.
61. Zhang J, Huan Y, Qian Y, Sun L, Ge Y. Multishot diffusion-weighted imaging features in spinal cord infarction. J Spinal Disord Tech 2005;18:277–282.
62. Maier SE. Examination of spinal cord tissue architecture with magnetic resonance diffusion tensor imaging. Neurotherapeutics 2007; 4:453–459.
63. Kurtzke JF. Rating neurological impairment in multiple sclerosis: an expanded disability status scale (EDSS). Neurology 1983;33: 1444–1452.